

# Forces on Bars in High-consistency Mill-scale Refiners: Effect of Consistency

**Dustin Olender and Peter Wild**

University of Victoria, BC, Canada

**Peter Byrnes**

Herzberg Institute of Astrophysics, Victoria, BC, Canada

**Daniel Ouellet**

Paprican, Vancouver, BC, Canada

**Marc Sabourin**

Andritz Inc., Springfield, OH, USA

## ABSTRACT

Laboratory experiments have shown that thermo-mechanical-pulp refiner process consistency can greatly affect the contact mechanics of bar-crossing impacts, specifically the shear forces. This effect was quantified using the equivalent tangential coefficient of friction,  $\mu_{teq}$ , of the recorded impact. In this work, arrays of piezo-based sensors capable of measuring normal and shear forces on bars, were installed in two high-consistency, mill-scale refiners, one operating as a primary stage, and the other, as a rejects stage. An increase in refining consistency, measured at the discharge, was observed to cause an increase in  $\mu_{teq}$  in the primary refiner, while no significant changes in  $\mu_{teq}$  were observed in the rejects refiner. These results confirm the existence of a relationship between  $\mu_{teq}$  and consistency at the mill-scale.

## INTRODUCTION

The contact mechanics that arise during bar-crossing impacts are responsible for inducing the stresses, and corresponding strains, that develop raw wood fibre into useful papermaking pulp. Enhancing our knowledge of the interactions that make up these impacts, and how they are affected by process variables, is therefore a necessary step to advancing refiner technology. Experiments by Senger and Ouellet [1] involving individual fibre bundles, or flocs, in a single-bar refiner have indicated that bar forces are dependent on floc consistency, floc grammage and bar edge sharpness. These results offered insight into previously unexplainable behavior, but investigation of these relationships in mill-scale refiners was restricted by lack of available measurement technology. This investigation is now possible with the development of a refiner force sensor (RFS) that replaces a small segment of refiner bar, and is capable of measuring normal and shear forces experienced during individual bar-crossing impacts. Bar forces from RFS tests in two mill-scale refiners under nominal operation have already been reported [2]. During the same installations, consistency within the refining zone was also varied in individual experiments. The principal goal of this work is to report on the effects of refining consistency on recorded bar forces in these two trials.

Goncharov *et al.* [3] first measured the rapid spike in force encountered as crossing bars meet in low-consistency refining, denoting it the *cornering force*. The authors recognized this cornering force as the primary driver of pulp quality. Senger and Ouellet [1] recently renewed interest in the shear forces encountered at bar edges, recognizing that they are directly responsible for working captured fibres. In investigating these shear forces, they define the equivalent tangential coefficient of friction,  $\mu_{teq}$ , as the ratio of average shear force to average normal force during a bar-crossing impact. This definition emphasizes that the shear force is not solely a linear friction component of the normal force, but also contains a significant cornering force component. During their tests in a single-bar refiner, the authors observed a dependency in  $\mu_{teq}$  only when floc consistencies were increased above approximately 35 %.

Above this value,  $\mu_{teq}$  was found to increase with increasing floc consistency. Senger and Ouellet note that this consistency matches the discharge consistency reported [4, 5] to induce a new energy-quality relationship in tests involving mill-scale refiners.

In the current research, RFS were installed in two high-consistency, single-disc refiners in separate field campaigns [2]. Tests were conducted in a 36 in. pressurized refiner, processing chips at the Andritz Pilot Plant, in Springfield, Ohio, and in a 45 in. rejects refiner at a Catalyst Paper Corp. mill, in Port Alberni, BC. Refining consistency in both campaigns was varied by altering the flow rate of the dilution water, and the speed of the dewatering press, to operational limits. A range of discharge consistencies between 20-55% was found in the primary stage refiner, while the best measurement of the range was between 20-27% in the rejects refiner. Experiments were performed over a two-day period in the primary stage refiner, and over a three-month period in the operational rejects refiner.

## EXPERIMENTAL

An earlier report [2] has already detailed the installation process in Springfield and Port Alberni, including photographs of sensor locations within the instrumented plate, as well as the plate pattern and relevant dimensions. These photos are included in the appendix of this report. In summary, the sensors were labelled S1, S2 and S3 in both trials, and were located at increasing radii, respectively, within the refining zone. S1 was the innermost sensor, while S3 was located in the outer region of the plate. Figure 1 shows the Port Alberni RFS identified as S3, (a) before installation, and (b) after removal from the plate following three months of operation. In Figure 1b the sensor housing is visibly tarnished and the material accumulated on its top surface is blackened pulp. All RFS probes were worn to the same height as surrounding bar, but generally experienced more rounding of their leading edge. Accelerated wear of the probes was expected, as the stainless steel used in their manufacture was considerably softer than the nickel-hardened plate material. RFS sensitivity was only marginally diminished after three months of operation.

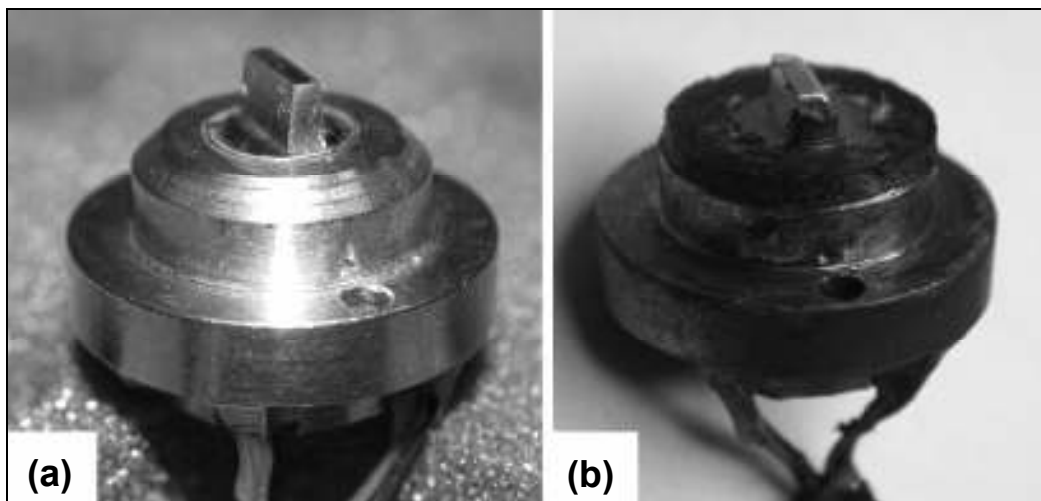


**Figure 1: Close-up of (a) outer sensor S3 prior to installation in Port Alberni, and (b) after three months of operation. The probe shows notable wear, along with tarnishing of the housing. A build-up of blackened pulp was also visible on the top surface.**

### Springfield and Port Alberni Trials

As noted, the experiments presented in this work were conducted during the same trials reported earlier by Olender *et al.* [2]. During the trials in Springfield and Port Alberni, all experiments were enumerated in chronological order. The same enumeration scheme used during the trials is adopted in this report.

The setup and experiments in Springfield took place over one week in early January 2005. Table 1 lists the process conditions of the experiments considered in this work. In these experiments, dilution flow rates were varied between 5 and 11 USGPM (19 and 42 l/m). At each dilution flow rate, two motor loads were targeted: 650 and 800 kW. After reaching equilibrium in each case, process conditions were held constant for between 15 to 30 s to allow a representative force signal and pulp sample to be acquired. The casing environment was held constant at a gauge pressure of 3.5 bar (350 kPa) and temperature of 148 °C. The refiner was run at a constant speed of 1900 rpm in hold-back mode during all tests. Hold-back mode is defined by the direction of rotor spin that causes crossing bars

to scissor radially inward. Spruce wood chips, having a moisture content of 48.6%, were used. Retention in pre-steaming tube was 120 s at a gauge pressure of 1 bar (100 kPa).

**Table 1: List of Springfield experiments.**

Sample ID	Target Motor Load (kW)	Actual Motor Load (kW)	Dilution Flow Rate (USGPM   l/m)	Specific Energy (kWh/t)	Plate Gap (mm)	Discharge Consistency (%)
A1	650	653	5   19	725	0.64	42.8
A2	800	794	5   19	899	0.36	54.9
A3	800	890	7   27	1018	0.36	44.2
A4	650	670	7   27	746	0.66	35.7
A5	650	639	9   34	708	0.89	27.1
A6	800	800	9   34	899	-	30.9
A7	800	834	11   42	949	0.86	25.2
A8	650	665	11   42	740	1.47	22.4
A9	650	616	9   34	679	1.19	27.0
A10	800	829	9   34	943	0.69	31.1
A11	800	800	7   27	932	-	37.7
A12	650	650	7   27	721	0.81	34.1
A13	650	642	5   19	711	0.64	46.4
A14	800	817	5   19	928	0.41	53.8

The trial in Port Alberni took place over a three-month period, starting in September and finishing in November of 2005. Following installation of the plate segment, a first trial consisting of two experiments was performed and is the focus of this work. In these two experiments, dilution flow rate and the pressure developed in the dewatering press were varied, while keeping other process variables constant, as shown in Table 2. Consistency of incoming reject pulp was approximately 28%. Production rate was held constant at approximately 60 odmt/d, and motor load at 3 MW. Once process conditions were stabilized, settings were held for approximately three minutes, as forces were recorded, and inlet and discharge pulp samples were taken.

**Table 2: List of Port Alberni experiments.**

Sample ID	Dilution Flow Rate (USGPM   l/m)	Pressure in Dewatering Press (psig)
A9	5   19	1500
A10		1600
A11		1700
A12		1800
A13	3   11	1700
A14	4.3   16	
A15	5.6   21	
A16	7   27	

No measurements of discharge consistency were taken from the samples recovered in the first Port Alberni trial, but measurements were taken during a later trial, which used the same operating conditions. The force data from this later trial is not included in this work because it is not expected to be representative, due to the accelerated bar wear on the probe tip. Values of discharge consistency in the later trial ranged from 20 to 27 % over the experiments. The historical average discharge consistency for the reject refiner under study is 33 % [6].

## SIGNAL CONDITIONING AND PROCESSING TECHNIQUES

The conditioning steps used to convert the two voltages from the RFS into normal and shear force signals are detailed in the previous report of these trials [2]. The same steps were taken in the analysis of these experiments. In brief, the voltages were first transformed into forces, using the method of superposition described elsewhere [7]. Secondly, the force signals were filtered to remove any magnitude distortion associated with operating near the RFS first natural frequency. Lastly, the signals were compensated for the loss of low-frequency components associated with piezoelectric transducer systems. This last step included inverse-filtering, and a final manual offset, which assumed the minima, or valleys of the force signals, are an accurate zero reference.

As noted in the previous report [2], software was written to identify and record individual bar-crossing impacts. Impact parameters, such as peak forces and  $\mu_{teq}$  were also catalogued. Impacts with a normal force below the 0.2 N system threshold (referred to as “low threshold” in the following sections) were discarded. Impacts with very high forces, representing less than 5 % of the total number of recorded impacts were isolated using a high force threshold (referred to as “high threshold”).

The averages reported in this work are based on data processed from three 5-second intervals spaced evenly throughout each experiment. Sigmaplot® 9.0 [8] graphing software was used to perform all regressions. S1 data for samples A2, A3 and A4 in Springfield were of poor quality, possibly due to a plate clash, and are, therefore, not included.

## RESULTS

### Springfield Trial

Figures 2, 3 and 4 present mean  $\mu_{teq}$  recorded by sensors S1, S2 and S3, respectively, for all Springfield experiments listed in Table 1. Results using both low and high threshold settings are included. All three sensors show an increase in  $\mu_{teq}$  with increasing consistency at the high threshold, but only the inner sensor S1 shows this relationship at the low threshold. Values of  $\mu_{teq}$  at the high threshold are also observed to be lower than those found using the low threshold in both S1 and S3.

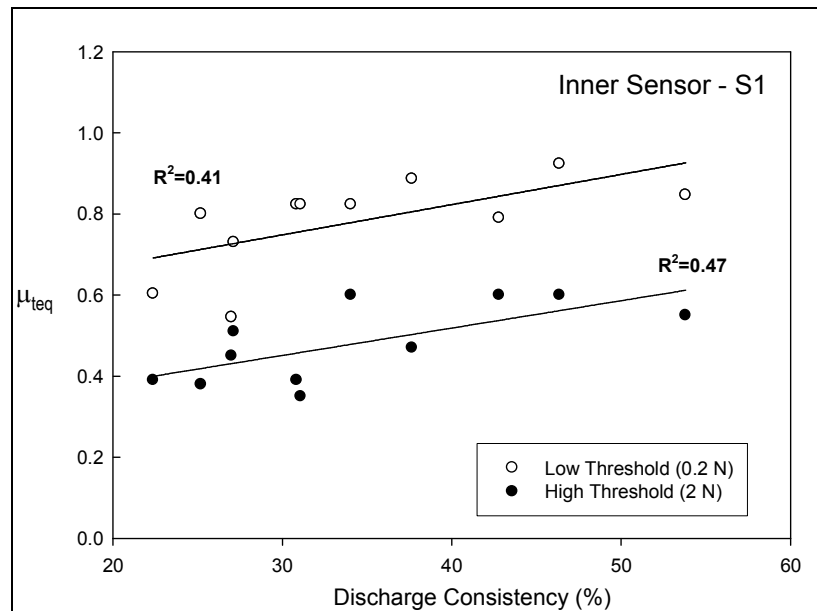


Figure 2: Effect of discharge consistency on  $\mu_{teq}$ , measured by inner sensor S1 in Springfield.

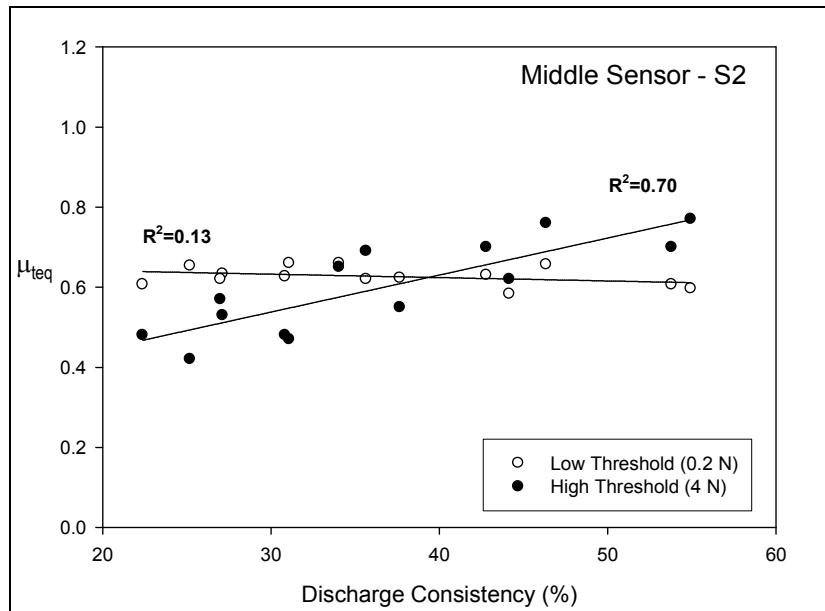


Figure 3: Effect of discharge consistency on  $\mu_{teq}$ , measured by middle sensor S2 in Springfield.

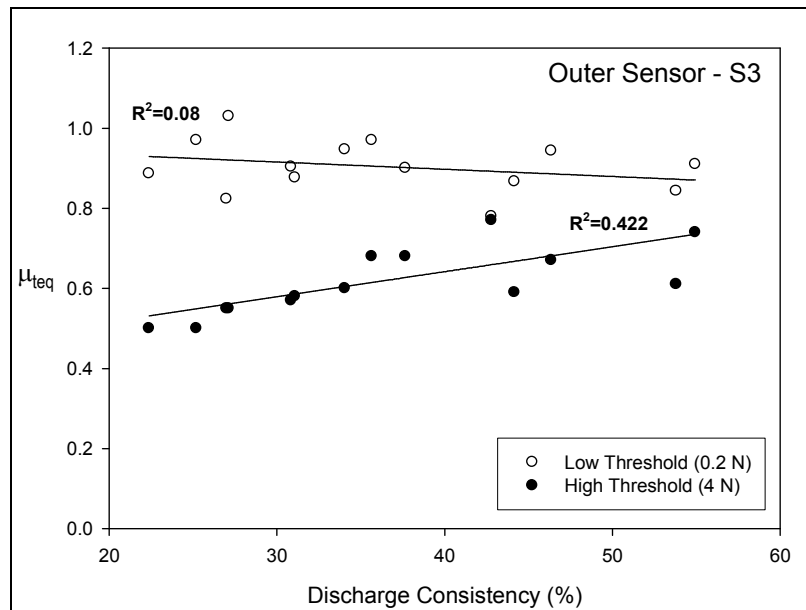
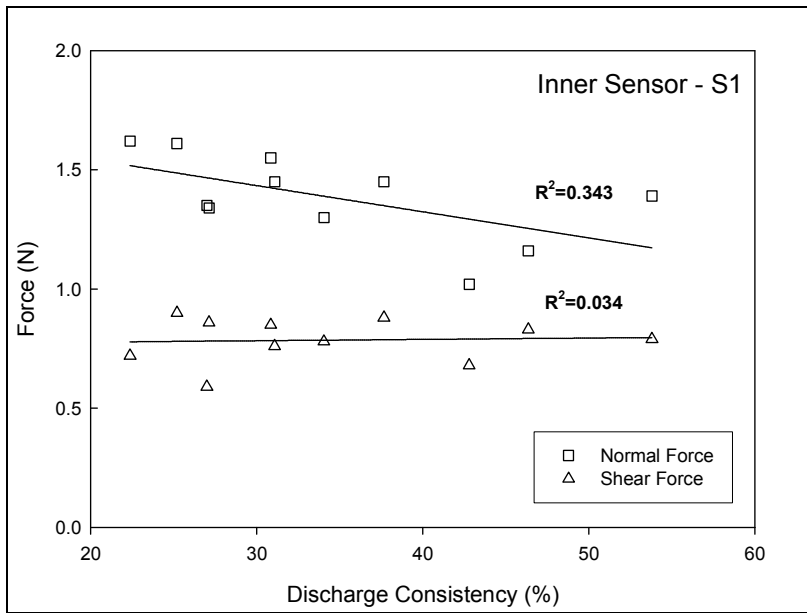
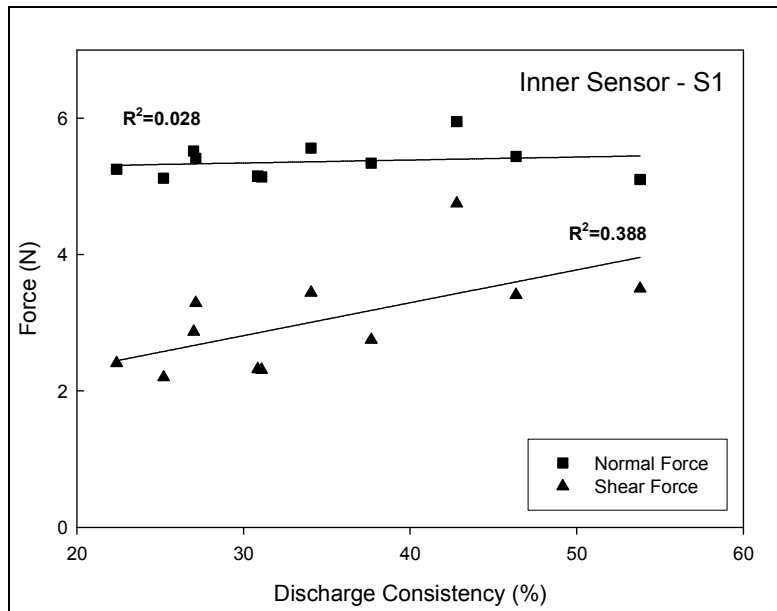


Figure 4: Effect of discharge consistency on  $\mu_{teq}$ , measured by outer sensor S3 in Springfield.

Figure 5 is a plot of the mean normal and shear forces recorded by sensor S1 at the low threshold. It is observed that the trend in  $\mu_{teq}$ , shown in Figure 2, is primarily caused by a drop in normal force. Figure 6 is a plot of the mean normal and shear forces recorded by sensor S1 at the high threshold. In this plot it is observed that the increase in  $\mu_{teq}$ , shown in Figure 3, is caused by a rise in shear force with increasing discharge consistency. A rise in shear force with discharge consistency is also responsible for the observed increase in  $\mu_{teq}$  at the high threshold setting for sensors S2 and S3. Mean normal force levels for the inner, middle and outer sensors were, respectively, 1.38 N, 1.52 N, and 0.93 N. Listed in the same sensor order, mean shear force levels were 0.78 N, 0.86 N, and 0.75 N.



**Figure 5: Effect of discharge consistency on mean forces recorded by inner sensor S1 in Springfield. Results were processed using the low threshold.**



**Figure 6: Effect of discharge consistency on mean forces recorded by inner sensor S1 in Springfield. Results were processed using the high threshold.**

Figure 7 plots mean values of  $\mu_{req}$  at the inner sensor with discharge consistency for the low threshold setting, but in this case separates the experiments by low and high motor loads. As seen in this figure,  $\mu_{req}$  at the low motor loads is observed to be more sensitive to the effects of consistency and records a higher coefficient of determination. This effect was not observed in the middle and outer sensors.

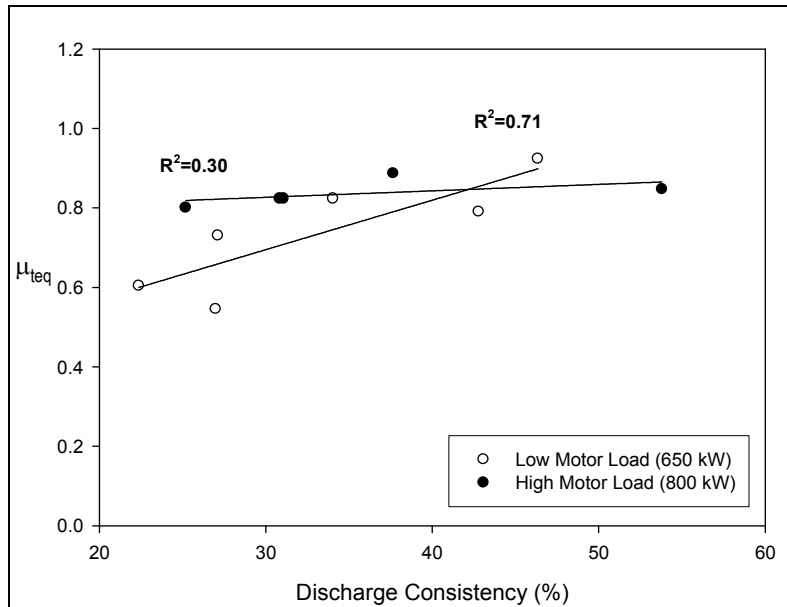


**Figure 7: Additional motor load effect on mean values of  $\mu_{teq}$  for the inner sensor S1 at low threshold. Low and high motor load experiments have been isolated and separate regressions performed.**

### Port Alberni Trial

Over the operating conditions tested, the sensors in Port Alberni measured no significant change in  $\mu_{teq}$  at either threshold setting. Mean values and standard deviations of  $\mu_{teq}$  at the low threshold were  $0.34 \pm 0.006$ ,  $0.64 \pm 0.015$ , and  $0.53 \pm 0.017$  for S1, S2 and S3, respectively. As mentioned previously, a measurement of discharge consistency was not performed on samples from the first trial, but was at a later date at the same operating conditions. This sampling took place on November 17, 2005, which was within one week of failure of the plates. Discharge consistencies measured in these samples ranged from 20 to 27 %.

### DISCUSSION

Senger and Ouellet [1] observed that an increase in consistency of a floc trapped between crossing bars leads to an increase in  $\mu_{teq}$  during the impact. The authors relate this behaviour to the ploughing component of friction. The shear force required to plough through a floc will increase with an increase in inter-fibre friction, which is dependent on the amount of water in the floc. This increase in  $\mu_{teq}$  was more pronounced with higher grammage (thicker) flocs subjected to the same normal force. In this case, the higher grammage flocs have more fibres in front of the crossing bar, and thus require a larger ploughing force to allow the floc to pass between crossing bars. It was proposed that these higher grammage interactions are therefore more sensitive to consistency based on the increased quantity of fibre between the bars.

The results of the current work support many elements of this hypothesis. The measurements taken in Springfield by sensor S1 show that impacts in the inner region of the refining zone experienced an increase in  $\mu_{teq}$  with increasing consistency. Sensors S2 and S3 in the middle and outer region also recorded this trend, but only for higher force impacts. The effect of grammage proposed by Senger and Ouellet offers a potential explanation. As the Springfield refiner was processing chip, inner sensor S1 would encounter more intact wood fibres, which would be thicker and thus higher grammage, than those encountered by sensors in the outer region. According to the work of Senger and

Ouellet, this would increase the ploughing component of friction and, accordingly, increase the likelihood of recording a change in  $\mu_{teq}$ .

As shown in Figure 5, the increase in  $\mu_{teq}$  recorded by the inner sensor at the low threshold is primarily driven by a drop in normal force. Senger and Ouellet performed their tests over similar ranges of normal forces, and found that the recorded trends in  $\mu_{teq}$  were primarily driven by an increase in the magnitude of the shear force. These findings, therefore, contradict this earlier work on this point. This behaviour is currently not understood.

In contrast, the high threshold findings for all sensors show the expected result, in that an increase in  $\mu_{teq}$  is caused principally by a rise in the shear force, which is attributed to an increase in ploughing force.

A further point of interest is the effect of motor load on the inner sensor's recorded increase in  $\mu_{teq}$  at the low threshold setting. As shown in Figure 7, by isolating the low and high motor load experiments it is clear that low motor loads show a higher degree of correlation with changes in consistency. Physical interpretation on this point is reserved until more data can be collected.

The lack of any significant change in  $\mu_{teq}$  in Port Alberni is not unexpected. The best available measurement of discharge consistencies encountered in this trial was below the 35 % threshold discovered by Senger and Ouellet known to affect  $\mu_{teq}$ . Although the measured values of discharge consistency are lower than anticipated, it is known that the discharge consistency of the refiner under study has a historical average (since 2003) of 33 % [6]; this is the lowest discharge consistency of the three reject refiners used at the mill. Further speculation as to the observed insensitivity of  $\mu_{teq}$  in Port Alberni should also include the small range of consistencies explored, and the potential of the stage of the fibre being processed to affect conditions.

## CONCLUSIONS

Bar force measurements were made by dual-axis sensors in the refining zones of two high-consistency, mill-scale refiners in separate field campaigns. Sensors were installed and tests were conducted in a 914 mm (36 in.) pressurized refiner, processing chips at the Andritz Pilot Plant, in Springfield, Ohio, and in a 1143 mm (45 in.) rejects refiner at a Catalyst Paper Corp. mill, in Port Alberni, BC. Variation of refining consistency was accomplished by altering dilution flow rates in both refiners. In the case of the rejects refiner, the speed of the dewatering press, which controls the consistency of incoming pulp, was also varied in a separate experiment.

Software was used to catalogue many thousands of individual bar-crossing impacts during each experiment from which a mean  $\mu_{teq}$  could then be calculated. Mean values of  $\mu_{teq}$  calculated solely from higher force impacts, which made up less than 5 % of total recorded impacts, were also explored.

An increase in discharge consistency from approximately 20 – 55 % in the primary stage refiner caused an increase in  $\mu_{teq}$  from approximately 0.5 to 0.8 in the innermost sensor. Higher force impacts showed a similar increasing trend, but at lower levels of  $\mu_{teq}$ . An increase in  $\mu_{teq}$  with discharge consistency for the middle and outer sensors was only observed for higher force impacts. This insensitivity over most of the impacts in the outer regions is thought to be due to the stage of fibre development. Thicker, or higher grammage, fibre bundles have shown an increased sensitivity to consistency in laboratory experiments, and the inner sensor is more likely to encounter thicker fibre bundles, such as shives.

The trends in  $\mu_{teq}$  at the inner sensor over the bulk of the impacts were shown to be caused by a drop in normal force, which was contrary to laboratory experiments. It was also noted that  $\mu_{teq}$  was more sensitive to consistency at



lower motor loads. No explanation for these behaviors is currently given, and it is hoped further experimentation will provide an answer. In contrast, the increase in  $\mu_{teq}$  in the higher force impacts behaved as expected. These trends were driven by a rise in shear force and attributed to an increase in the cornering force necessary during ploughing of the fibre material.

In the Port Alberni trial, no significant change in  $\mu_{teq}$  was observed over the experiments. The closest measurement of the range of discharge consistencies encountered in these experiments is between 20-27 %. This is within the range, below 35 %, where  $\mu_{teq}$  was observed in laboratory experiments to be insensitive to changes in consistency. This is considered to be an important factor in the current findings, and likely resulted in the observed insensitivity at Port Alberni.

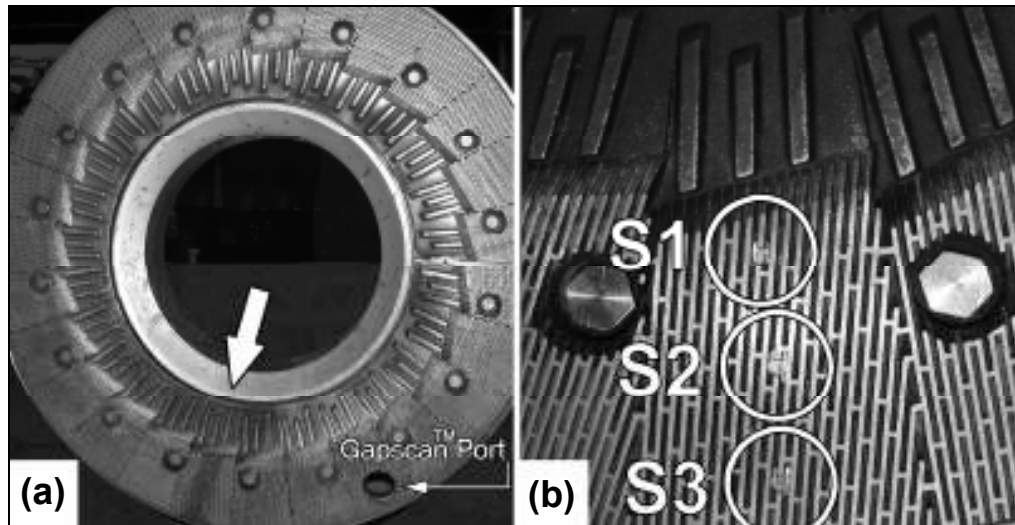
## ACKNOWLEDGEMENTS

The authors gratefully acknowledge funding provided by the Natural Sciences and Engineering Research Council, Andritz Ltd., and Paprican; and access to experimental and commercial facilities provided by Andritz Ltd., and Catalyst Paper Corp.. The authors would also like to thank John Senger for valuable discussions during the campaigns and to Ingunn Omholt for support and discussion throughout the project.

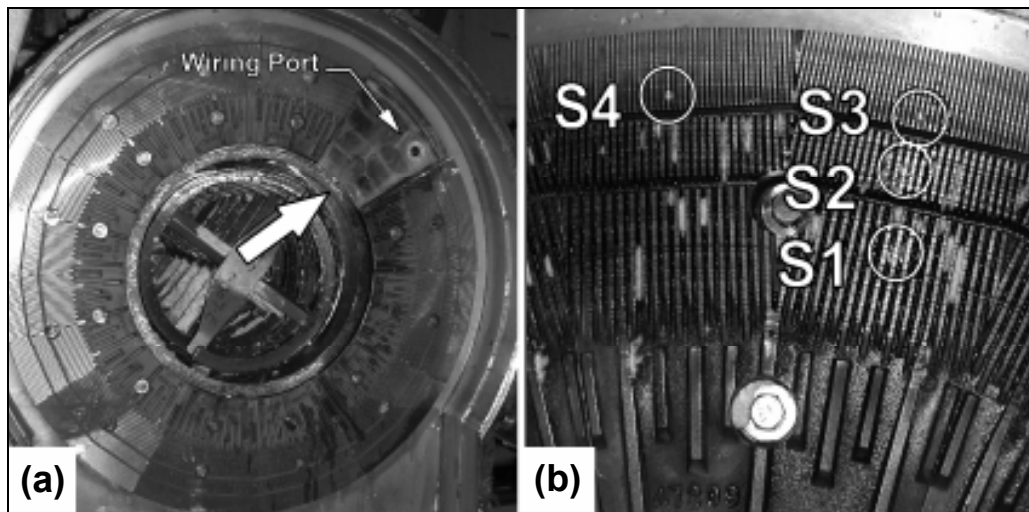
## REFERENCES

1. SENGER, J., AND D. OUELLET, "Factors Affecting the Shear Forces in High-consistency Refining," J. Pulp Paper Sci., 28(11):364 – 368 (2002).
2. OLENDER, D., WILD, P., BYRNES, P., OUELLET, D. AND M. SABOURIN, "Forces on bars in high-consistency mill-scale refiners: trends in primary and rejects stage refiners," PAPTAC 93rd Annual Meeting (2007).
3. GONCHAROV, V.N., "Force Factors in a Disk Refiner and their Effect on the Beating Process," Bumazh. Promst. English Trans., 12(5):12-14 (1971).
4. MURTON, K.D., "Effect of primary stage consistency on TMP pulp quality and energy consumption," 51<sup>st</sup> Appita Annual General Meeting, s.l.:87-94 (1997).
5. ALAMI, R., BOILEAU, I., HARRIS, G., LACHAUME, J., KARNIS, A., MILES, K.B., AND A. ROCHE, "Impact of refining intensity on energy reduction in commercial scale refiners: effect of primary stage consistency," Tappi J., 80(1):185-193 (1997).
6. SASAKI, K., Process Specialist, Catalyst Paper Corp., Private communication, (August, 2006).
7. SIADAT, A., BANKES, A., WILD, P.M., SENGER, J., AND D. OUELLET, "Development of a Piezoelectric Force Sensor for a Chip Refiner," Proc. IMechE, Part E, Journal of Process Mechanical Engineering, 217:133-140 (2003).
8. SYSTAT SOFTWARE, "Sigmaplot 9.0 User's Manual," ISBN: 1568272510, 852 pages (2004).

APPENDIX



A 1: Location of instrumented plate segment, and force sensors in Springfield trial. (a) Instrumented segment in position. (b) Location and identification of the sensors in instrumented plate.



A 2: Location of instrumented plate segment, wiring port and force sensors in Port Alberni trial. (a) Vacant segment position, just prior to installation of the instrumented plate. (b) Location and identification of the sensors in the instrumented plate.

# Refiner Force Sensor Project:

**Paper 1:** Forces on Bars in High-consistency Mill-scale refiners: Effect of Consistency

**Paper 2:** Refiner Plate Clash Detection Using an Embedded Force Sensor

Presented by: Dustin Olender

Co-authors: Peter Wild, Paul Francescutti, Peter Byrnes, Daniel Ouellet, and Marc Sabourin

Partners:



University  
of Victoria



Paprican

ANDRITZ



NSERC  
CRSNG

IMPC 2007



# Outline

## ◀ Paper 1: Effect of Consistency

- Introduction
- Experiments
- Signal Processing
- Results and Discussion

## ◀ Paper 2: Plate Clash Detection

- Introduction
- Signal Processing
- Results and Discussion



# Introduction: Background

## ◀ Laboratory single-bar refiner:

- Found a relationship between impact shear forces and floc consistency
- Defined the *equivalent tangential coefficient of friction*  $\mu_{teq}$  as average shear divided by average normal force
- Flocs with consistencies above 35% were shown to have positive correlation with  $\mu_{teq}$



# Introduction: RFS4 Trials

## ◀ Springfield, OH



- Qualify RFS4 in pressurized 36-1CP refiner
- Test consistency

## ◀ Port Alberni, BC



- Qualify long-term operation of RFS4 in 45-1B
- Test consistency



Close-up of RFS4 installed in 45-1B in Port Alberni



# Outline

## ◀ Paper 1: Effect of Consistency

- Introduction
- Experiments
- Signal Processing
- Results and Discussion

## ◀ Paper 2: Plate Clash Detection

- Introduction
- Signal Processing
- Results and Discussion



# Experiments: Installation

Springfield, OH



Installation of instrumented 36604 plate



◀ RFS installed through rear of plate





# Experiments: Installation

Springfield, OH



► 7 o'clock position



Location of instrumented plate in 36-1CP stator



# Experiments: Installation

Springfield, OH



- ▶ 3 sensors positioned evenly throughout refining zone



Identification of RFS in 36604 plate



# Experiments: Trial Plan

Springfield, OH



- ◀ Spruce chips were refined
- ◀ Four (4) dilution flow rates, at two (2) different motor loads
- ◀ Dilution flow rate: 5 – 11 USGPM
- ◀ Motor loads: 650 kW – 800 kW
- ◀ Refiner speed: 1900 RPM

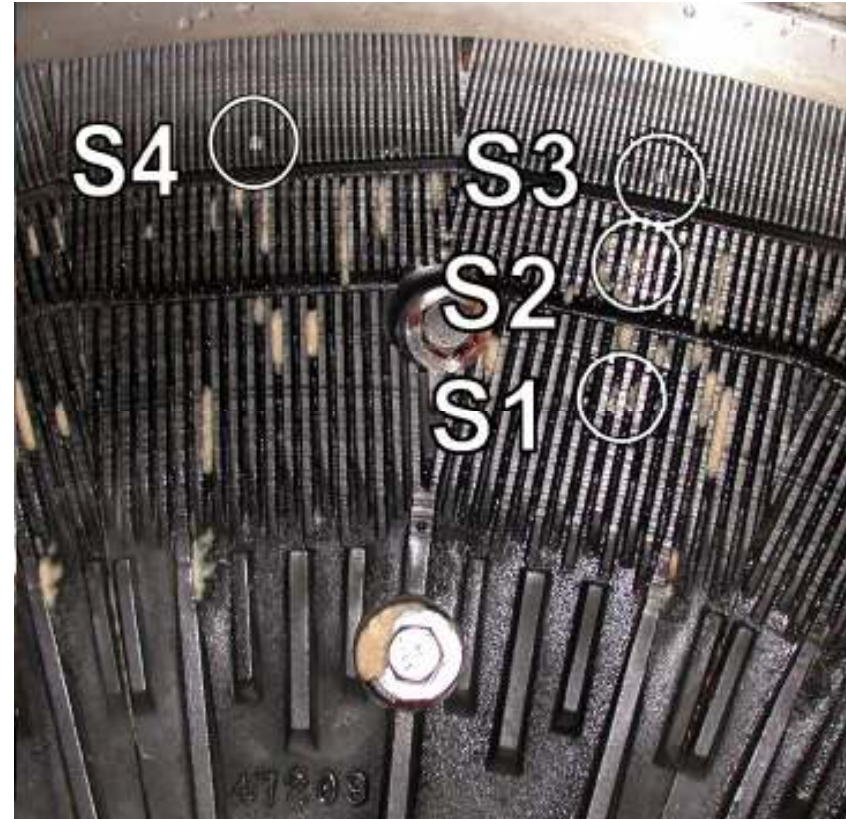


# Experiments: Installation

Port Alberni, BC



- ▶ 3 sensors +1 redundant at outer radius



Identification of RFS in 47209 plate



# Experiments: Trial Plan

Port Alberni, BC



- ◀ CTMP Rejects Pulp
- ◀ Dilution flow rate(3 – 7 USGPM) and speed of dewatering press at constant motor load (3 MW)
- ◀ Refiner speed: 1800 RPM



# Outline

## ◀ Paper 1: Effect of Consistency

- Introduction
- Experiments
- **Signal Processing**
- Results and Discussion

## ◀ Paper 2: Plate Clash Detection

- Introduction
- Signal Processing
- Results and Discussion



## Signal Processing:

- ◀ Software used to isolate and catalogue individual bar-crossing
- ◀  $\mu_{teq}$  calculated for each bar-crossing
- ◀ Mean  $\mu_{teq}$  calculated from three 5-second samples (100 000s of bar-crossings)



# Outline

## ◀ Paper 1: Effect of Consistency

- Introduction
- Experiments
- Signal Processing
- Results and Discussion

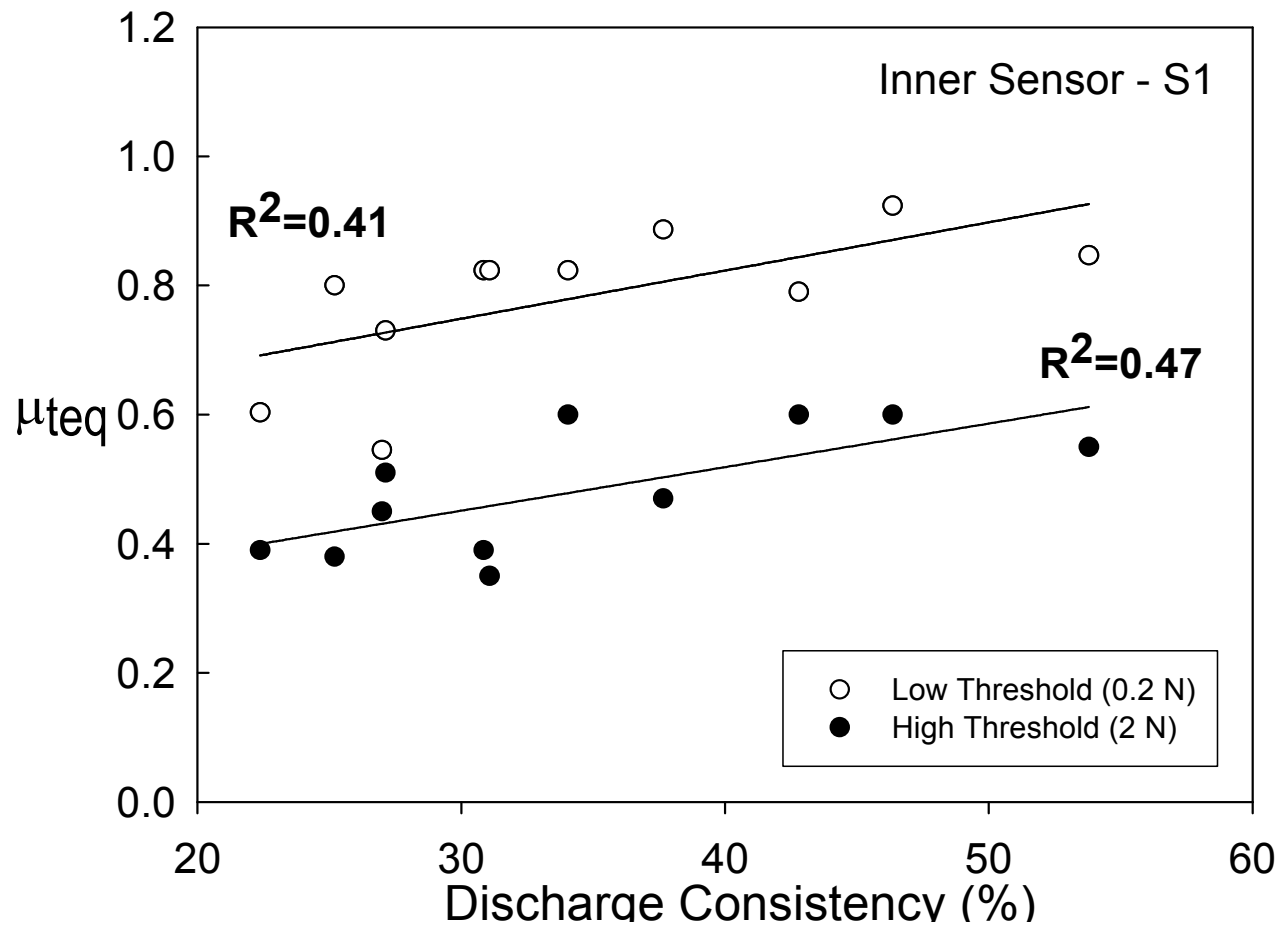
## ◀ Paper 2: Plate Clash Detection

- Introduction
- Signal Processing
- Results and Discussion



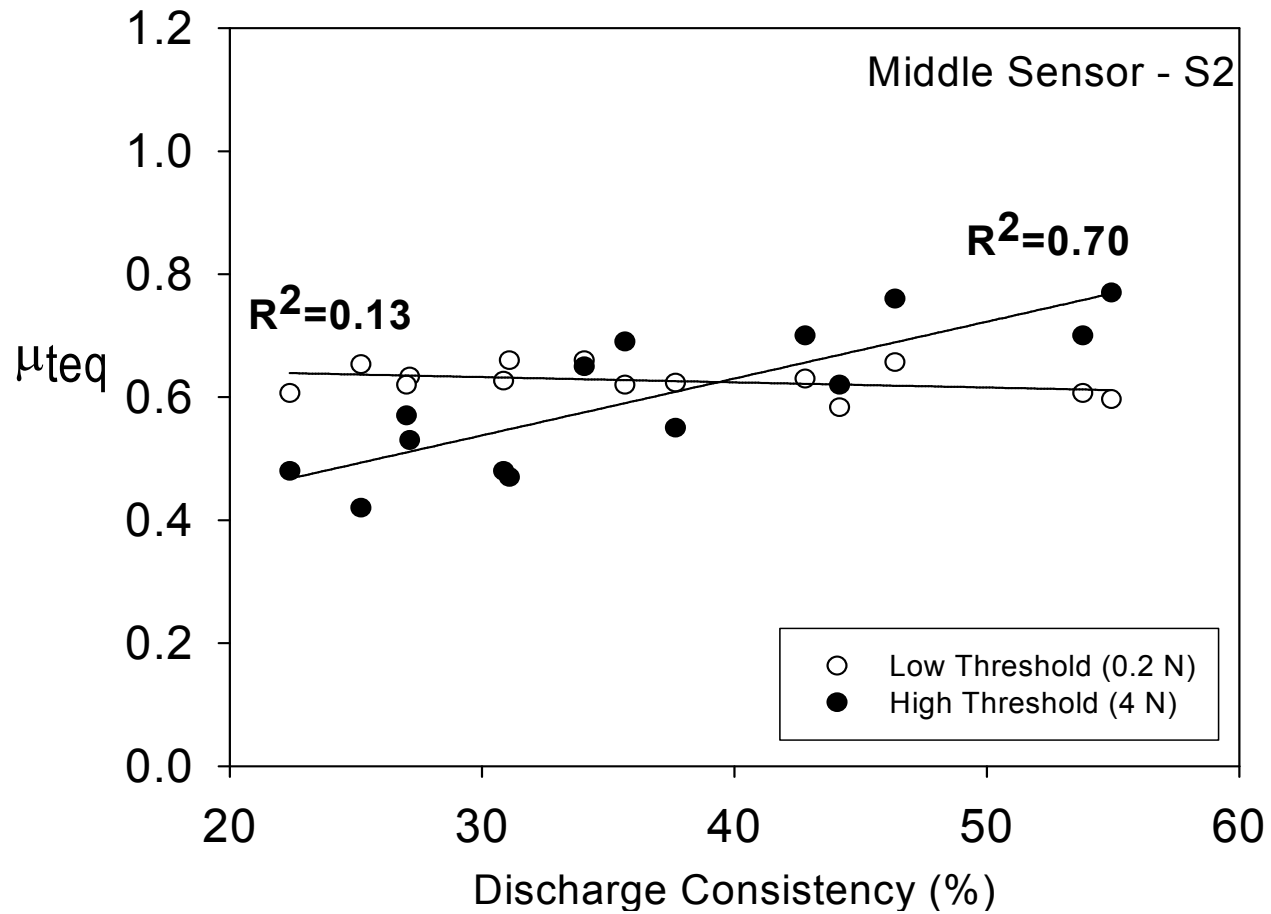


# Results: Springfield



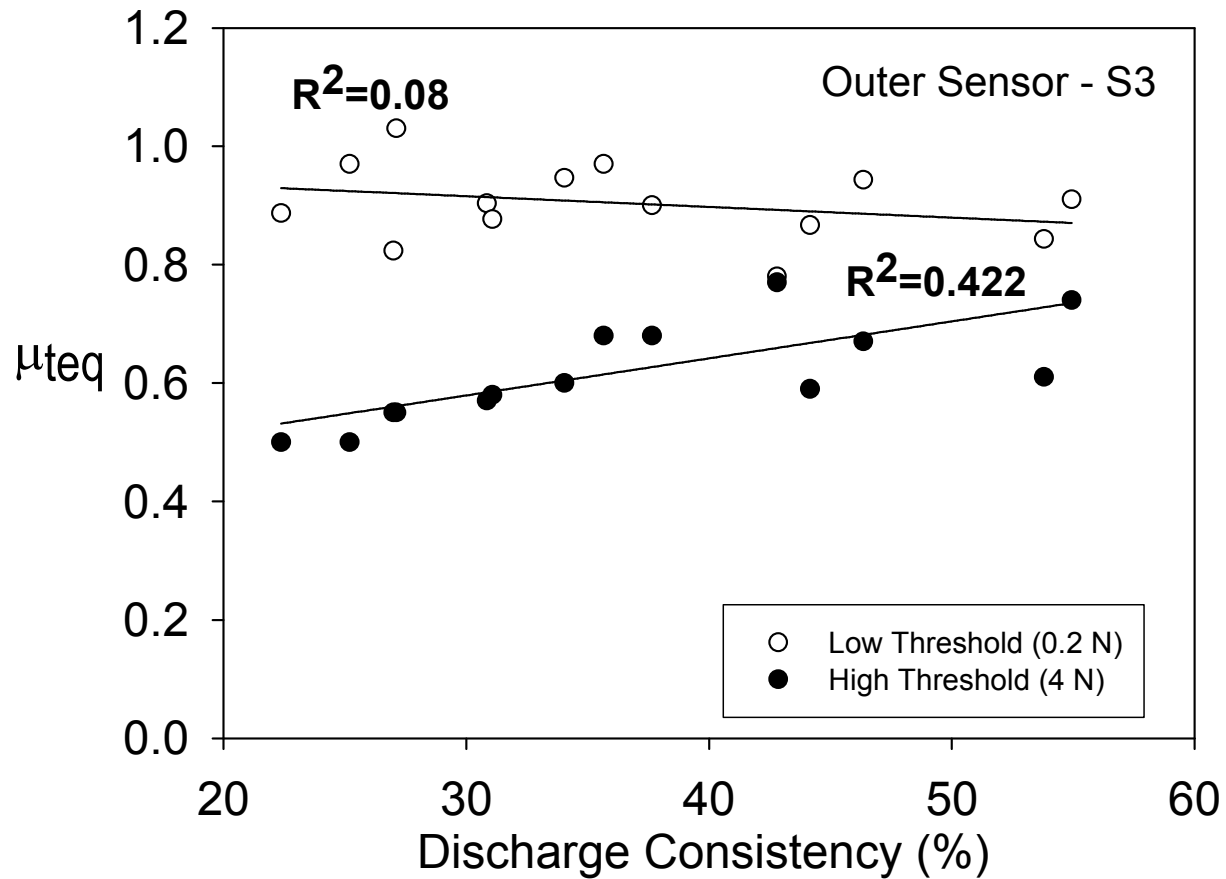


# Results: Springfield



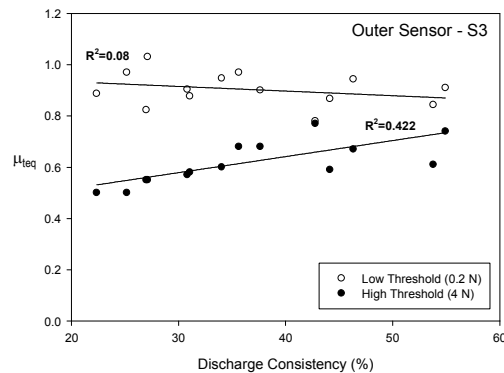
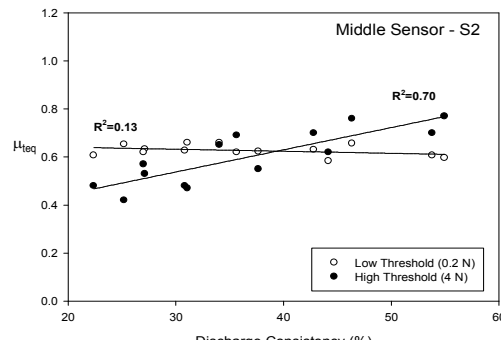
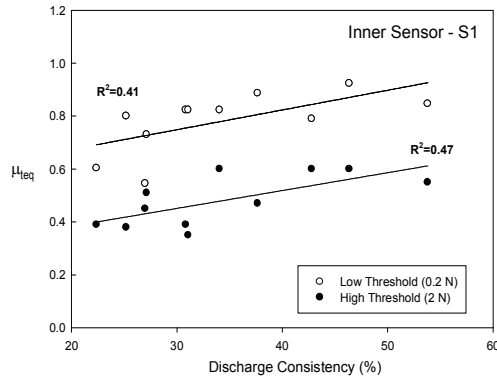


# Results: Springfield





# Discussion: Springfield



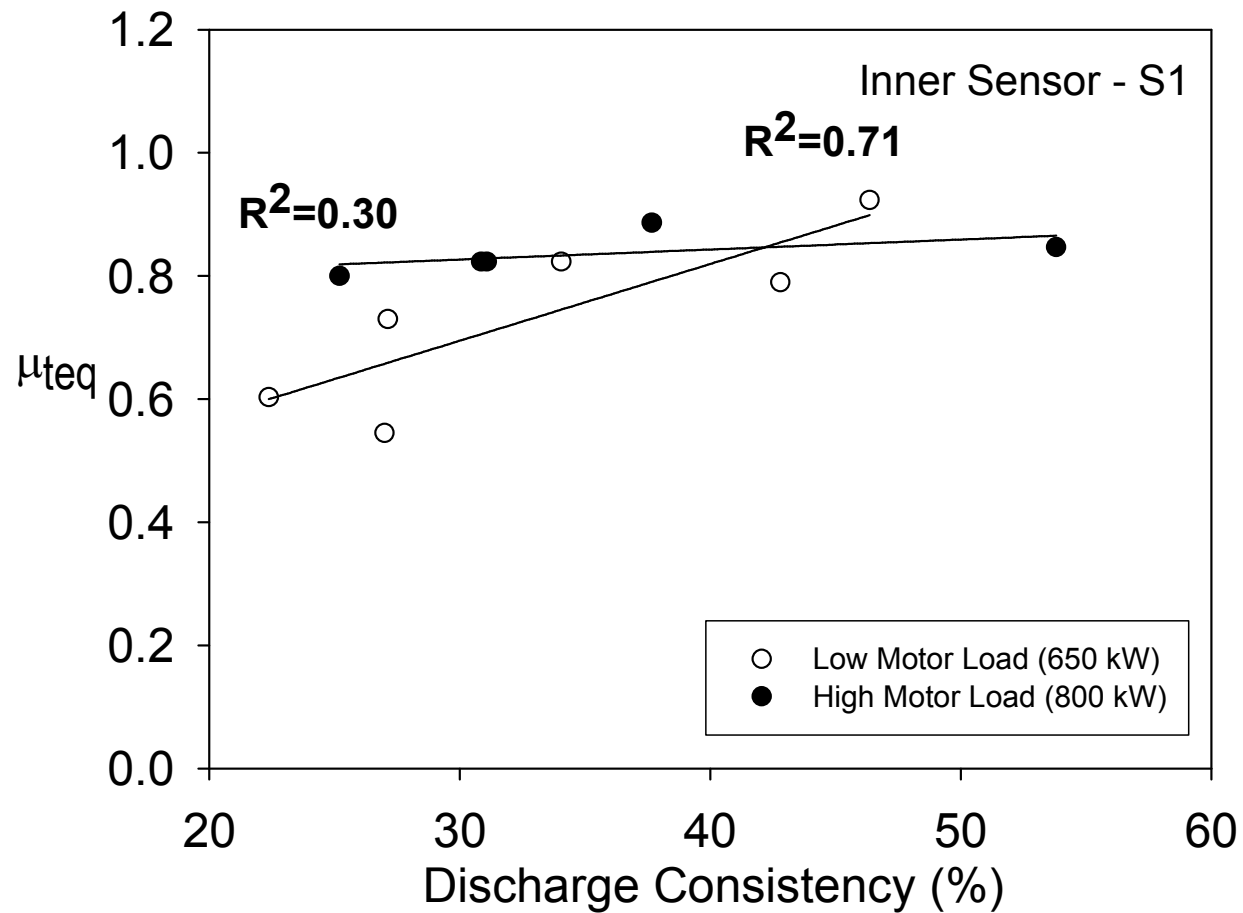
## Inner Sensor Sensitivity:

◀ Thicker grammage flocs were shown to increase sensitivity to  $\mu_{teq}$  in laboratory experiments

◀ Inner sensor encounters thicker, more intact fibre bundles, such as shives

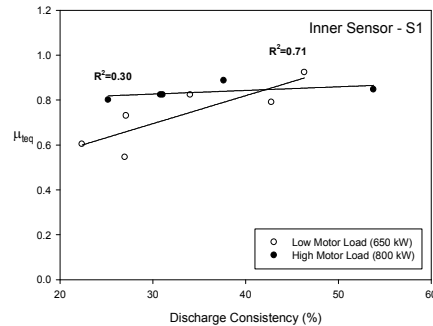


# Results: Springfield





# Discussion: Springfield



## Low Motor Loads:

◀ Low motor loads saw increased sensitivity to  $\mu_{teq}$

◀ More research is necessary



## Results: Port Alberni

- ◀ No significant changes in  $\mu_{teq}$  recorded over experiments
- ◀  $\mu_{teq}$  recorded at inner, middle and outer sensors: 0.34, 0.64, and 0.53.



## Discussion: Port Alberni



### **No Change in $\mu_{teq}$ :**

- ◀ Recorded discharge consistencies (20-27%) below 35% threshold
- ◀ Shear forces unchanged in flocs with consistency below 35% in laboratory
- ◀ Small range of consistencies could also be a factor





# Outline

## ◀ Paper 1: Effect of Consistency

- Introduction
- Experiments
- Signal Processing
- Results and Discussion

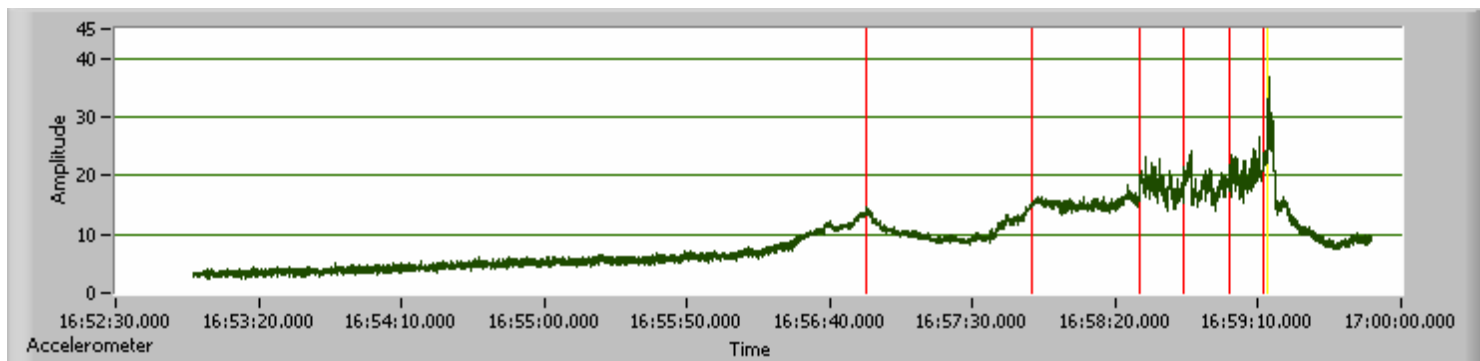
## ◀ Paper 2: Plate Clash Detection

- Introduction
- Signal Processing
- Results and Discussion



# Introduction: Current Plate Protection System

- ◀ Current system consists of two alarms based on data collected from an accelerometer mounted on the refiner.
  - **Alert:** The plates are opened when the accelerometer signal exceeds a set threshold.
  - **Danger:** The plates are opened when the accelerometer signal exceeds a running average by a set threshold.





# Outline

## ◀ Paper 1: Effect of Consistency

- Introduction
- Experiments
- Signal Processing
- Results and Discussion

## ◀ Paper 2: Plate Clash Detection

- Introduction
- Signal Processing
- Results and Discussion



# Signal Processing: Detection Methods

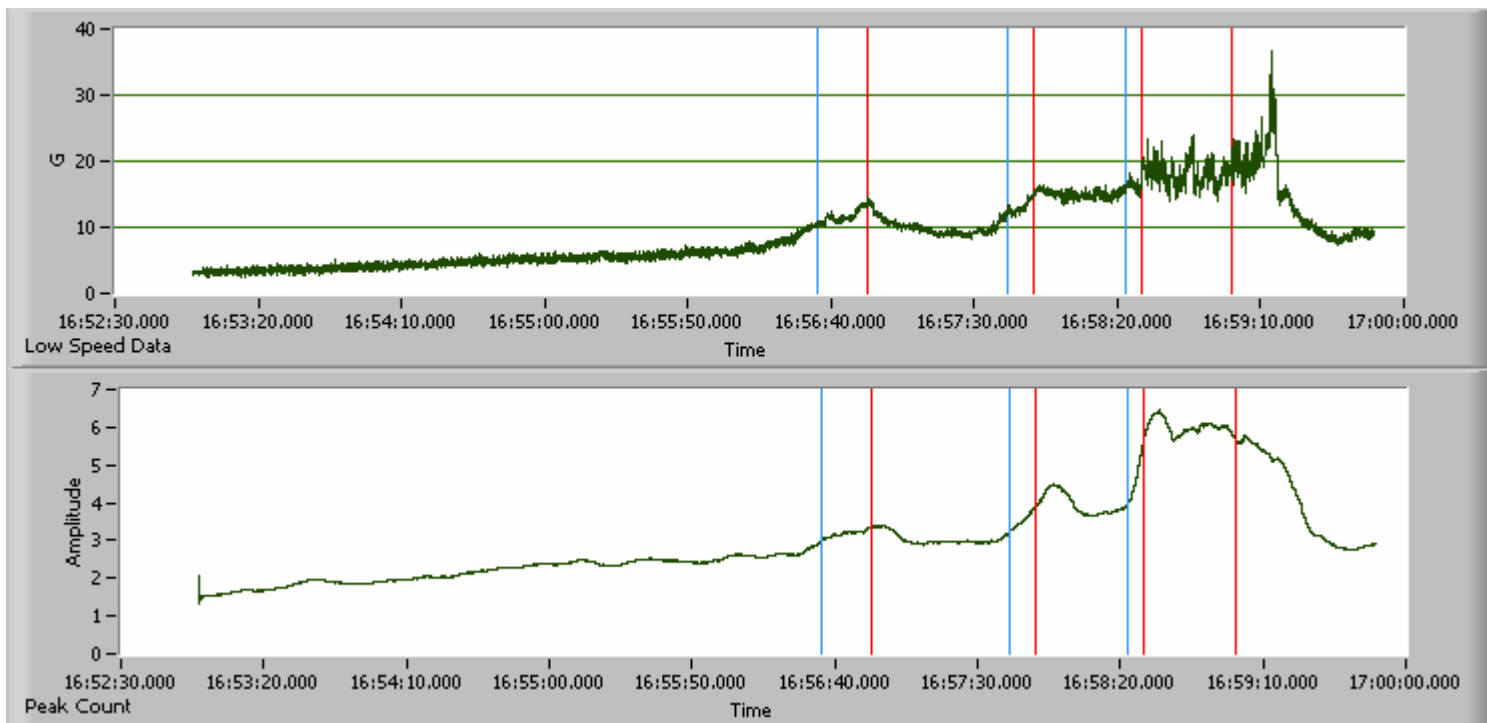
- ◀ Using the RFS data to generate a trend which can be monitored for clash detection.
  - Reduce sample rate and rectify data.
  - Calculate the running average of the RFS data for each data curve (2 per sensor).
  - Compare the curve to a dynamic threshold.



# Signal Processing: Detection Method Cont'd

## ◀ One sensor used to predict clash

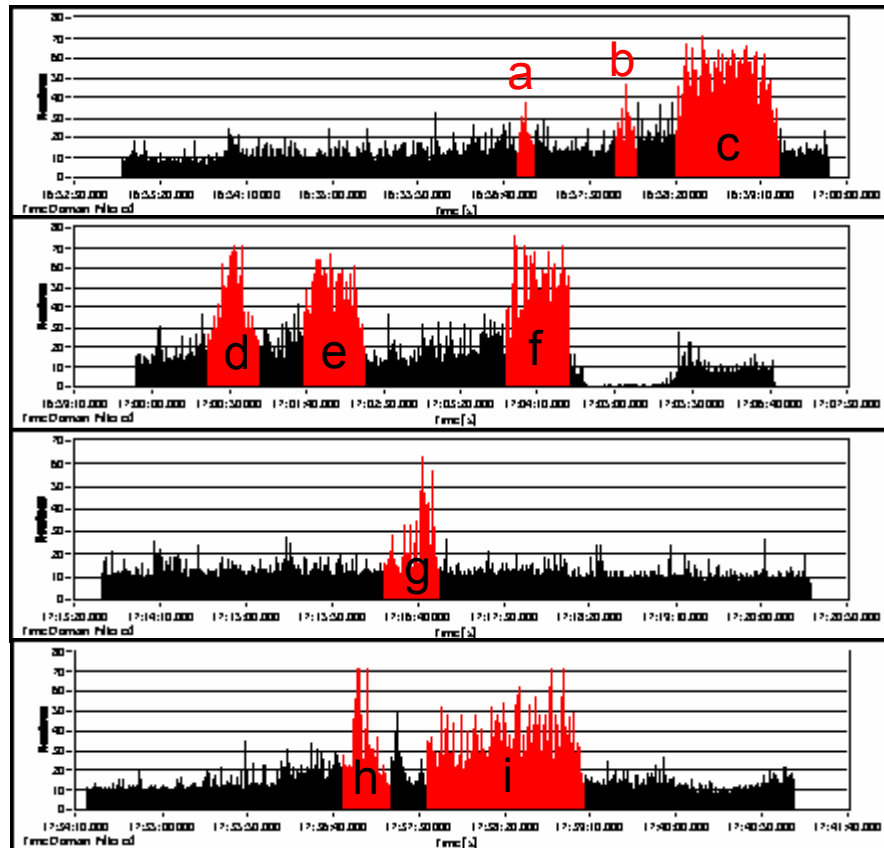
- Curve generated from average of Normal and shear force.
- Threshold is based a 15 s running average.





# Results: Clash Detection

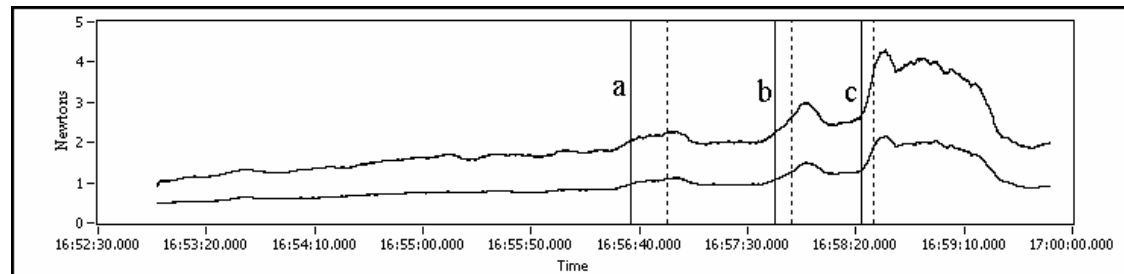
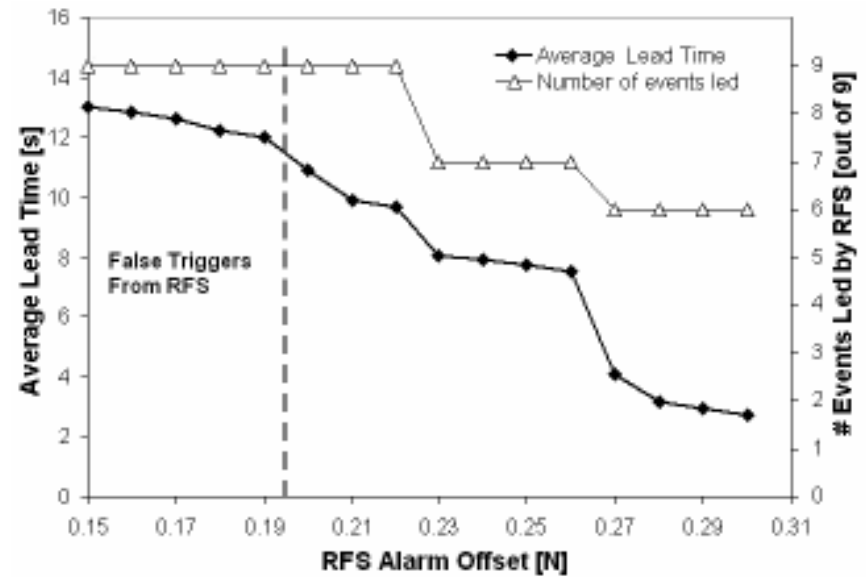
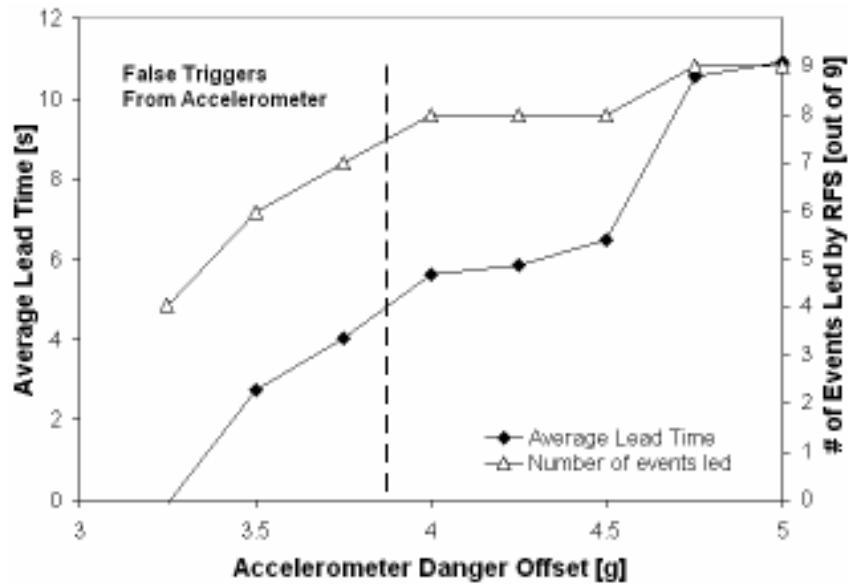
◀ RFS clash detection was able to predict all clash events before the accelerometer system.



Event	RFS lead [s]
a	12.9
b	9.3
c	6.1
d	7.5
e	24.7
f	11.2
g	15.9
h	21.86
i	8.71
<b>average</b>	<b>10.9</b>



# Results: Sensitivity Study





## Conclusions: Clash Detection

- ◀ The RFS sensor was able to predict a clash several seconds before the current accelerometer-based system.
- ◀ Sensitivity study showed that the accelerometer could not match the RFS clash detection without producing false triggers.





Thank-you  
&  
Questions?



# Springfield Trial Plan

Σαμπλε ΙΔ	Ταργετ Μοτορ Λοαδ (κΩ)	Προδ. Ρατε (τ/δ)	Σπεχιφιχ Ενεργγψ (κΩη/τ)	Πλατε Γαπ (μμ)	Δισχηαργε Χονσιστ. (%)
A15	550	21.1	562	0.76	
A16	650		673	0.56	
A17	750		721	0.43	
A18	850		899	0.25	
A19	450	18.4	505	1.07	
A20	550		626	0.94	
A21	650		702	0.74	
A22	750		891	0.46	
A23	600	26.4	521	0.94	
A24	700		620	0.64	
A25	800		701	0.53	
A26	900		796	0.36	

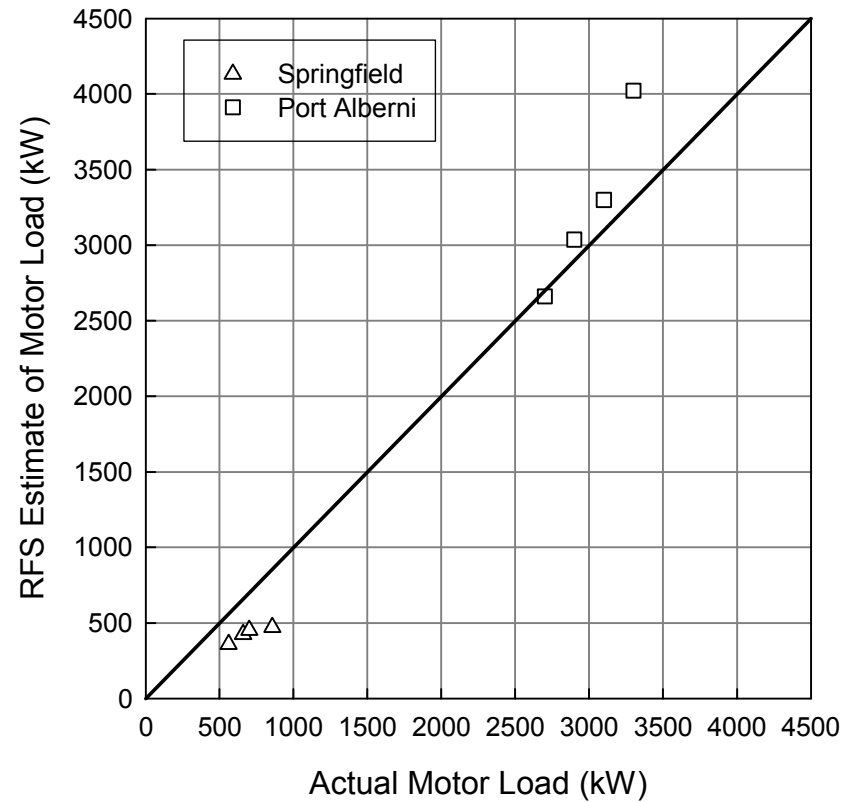


# Port Alberni Trial Plan

Σαμπλε ΙΔ	Μοτορ Λοαδ (κΩ)	Προδ. Ρατε (οδμτ/δ)	Σπεχιφιχ Ενεργψ (κΩη/τ)
A1	2700	61.2	1055
A2	2900		1137
A3	3100		1216
A4	3300		1294
A5	3000	55.0	1309
A6		59.3	1214
A7		61.4	1173
A8		65.5	1099



# Shear Work: Power Estimate





# Experiments: Installation

Port Alberni, BC



Wire routing to 45-1B refiner at Port Alberni



- ◀ Pre-installation of ancillary equipment one week prior
- ◀ Main installation during routine plate change



# Experiments: Installation

Port Alberni, BC



◀ Instrumented plate installed at 2 o'clock

Stator awaiting plate on 45-1B refiner